Proc. Indian Acad. Sci. (*Chem. Sci.*), Vol. 115, Nos 5 & 6, October–December 2003, pp 561–571

Hydrogen transfer reaction of cyclohexanone with 2-propanol catalysed by CeO_2-ZnO materials: Promoting effect of ceria[¶]

BRAJA GOPAL MISHRA, G RANGA RAO* and B POONGODI
Department of Chemistry, Indian Institute of Technology Madras,
Chennai 600 036, India
e-mail: grrao@iitm.ac.in

Abstract. Ce–Zn–O mixed oxides were prepared by amorphous citrate process and decomposition of the corresponding acetate precursors. The resulting materials were characterised by TGA, XRD, UV-Vis-DRS, EPR, SEM and surface area measurements. XRD and DRS results indicated fine dispersion of the ceria component in the ZnO matrix. EPR results clearly indicate the presence of oxygen vacancy and defect centres in the composite oxide. Addition of CeO_2 to ZnO produced mixed oxides of high surface area compared to the pure ZnO. Hydrogen transfer reaction was carried out on these catalytic materials to investigate the effect of rare earth oxide on the activity of ZnO. Addition of ceria into zinc oxide was found to increase the catalytic activity for hydrogen transfer reaction. The catalytic activity also depended on the method of preparation. Citrate process results in uniformly dispersed mixed oxide with higher catalytic activity.

Keywords. Cyclohexanone; ceria; ZnO; diffuse reflectance; EPR.

1. Introduction

In the field of catalysis, much effort has been spent in the preparation, characterisation and application of ceria and ceria based mixed oxide materials for automotive exhaust catalysis and oxidation of environmental pollutants.[1–5] The influence of the redox properties of ceria on several reactions has also been investigated systematically.[2,3,6–8] The number of effective redox sites and their ability to exchange oxygen can be manipulated by incorporating transition metal ions into the ceria lattice and promoted by noble metals dispersed on ceria particles.[1–4] Zirconia-incorporated ceria is a good example which shows enhanced reducibility in the presence of noble metals such as Rh, Pt and Pd.[3,4] While the role of ceria as a redox promoter has been well established, there is much scope to investigate the acid base properties of ceria-based materials. A few reports have appeared on this aspect.[6–12] The ceria-based mixed oxides studied recently for various organic transformations include CeO_2–MgO,[7,8] CeO_2–NiO,[9] CeO_2–SnO_2[11] and CeO_2–ZrO_2.[6,13,14] In some of these systems the promoting effect of ceria is attributed to both redox and mild acid–base properties of the ceria component.[6–8] The mobility of the surface oxygen in ceria has also been correlated with the catalytic activity for alcohol transformation.[15] Among the predominant oxide materials, ceria seems to show the highest surface oxygen mobility which has been correlated well with the basicity data available from CO_2 chemisorption studies.[16] The extent of dispersion, surface area and

[¶]Dedicated to Professor C N R Rao on his 70th birthday
*For correspondence

the substitution of suitable metal ions are some of the major factors affecting the reducibility and catalytic activity of ceria related materials. Two distinctly different reduction features have been observed in the TPR profiles of high surface area ceria samples related to the bulk and surface reductions while the sintered ceria shows only one reduction feature at higher temperature due to bulk reduction.[1,3,4] Catalytic chemistry of ceria continues to be an important and promising area of research in oxide catalysis and a voluminous knowledge on various aspects of this material has recently been published.[17] In the present study, we discuss the promoting effect of highly dispersed ceria in the ZnO matrix. For this purpose a relatively lower concentration of ceria (10 mol%) has been chosen in the CeO_2–ZnO composite catalyst. Since the preparation procedure is important for the final property of the composite oxide, we have adopted amorphous citrate process to prepare CeO_2–ZnO mixed oxide materials. This method is employed successfully for the preparation of high surface area mixed oxides.[8,10] The CeO_2–ZnO and ZnO materials have also been prepared by conventional method of decomposition from the acetate salts to demonstrate the effect of preparative conditions on the catalytic activity of the composite oxide. Hydrogen transfer reaction of cyclohexanone with isoproponol has been selected as a model reaction to study the catalytic activity of the composite oxides of ceria.

Catalytic hydrogen transfer reaction involves the reduction of multiple bonds in presence of a hydrogen donor and a catalyst.[18,19] The use of a hydrogen donor in place of molecular hydrogen has potential advantages in terms of mild reaction conditions and regioslectivity to a particular product.[20,21] The most widely employed hydrogen donors are alcohols (mainly secondary alcohols), cyclohexane, formic acid and hydrazine.[18] Noble metal catalysts are highly active for the transformation and the reaction is carried out under ambient or reflux conditions. The noble and transition metal complexes have also been used as catalysts for hydrogen transfer reaction in homogeneous conditions.[19] Heterogeneous catalytic reduction in liquid phase is generally carried out over noble metals either in finely divided form or dispersed on carriers such as carbon, $CaCO_3$, $BaSO_4$ and asbestos.[18] The vapour-phase transfer hydrogenation has been carried out over MgO,[22] ZrO_2, MgO/B_2O_3,[21] $Zr_{0\cdot8}(M)_{02}O_2$ (M = Fe, Co, Ni, Cu, Cr and Mn),[20] CeO_2–ZrO_2,[13] hydrotalcite like precursors,[23] heteropolyacids[24] and hydrous zirconia[25,26] which display basic or amphoteric characters. The reaction mechanism is similar to the Meerwein–Ponndorf–Verley type reduction and is thought to proceed in a concerted manner on the oxide surface involving the formation of a six member cyclic intermediate. The hydrogen acceptor and the donor are adsorbed on adjacent acidic and basic sites facilitating the hydrogen transfer reaction. The transfer of the hydride ion from the donor to the acceptor has been found to be the rate-determining step for the reaction.[26]

2. Experimental

CeO_2(10%)–ZnO mixed oxide (denoted as Ce–Zn–O-cit) and pure ZnO (denoted as ZnO-cit) were prepared from cerium (III) nitrate hexahydrate ($Ce(NO_3)_3$ $6H_2O$), zinc nitrate hexahydrate ($Zn(NO_3)_2{\cdot}6H_2O$) and citric acid monohydrate ($C_6H_8O_7.H_2O$) (all from SD Fine Chemicals, India) by amorphous citrate process. A solid mixture of cerium and zinc nitrates of desired molar ratio was mixed with an equimolar amount of citric acid and heated at 60°C to form a uniform melt. The molten mixture was then evacuated at the same temperature until it forms an expanded spongy solid material. It was then heated at 160°C for 2 h to decompose nitrates and calcined at 500°C for 3 h to obtain pure and

mixed oxide components. For comparative purpose, ZnO (denoted as ZnO-dec) and CeO_2(10%)–ZnO (denoted as Ce–Zn–O-dec) were prepared from the decomposition of corresponding acetate salts. For the preparation of the CeO_2(10%)–ZnO, cerium acetate and zinc acetate were mixed in the desired molar ratio and dissolved in minimum amount of water to form a paste. The paste was dried overnight at 150°C and calcined at 500°C for 3 h. The powder X-ray diffraction patterns of the samples were recorded using Philips X-ray diffractometer using Ni-filtered CuK_a radiation (λ = 1·5418 Å). Thermogravimetry analysis of the citrate precursors was done using Perkin–Elmer TGA-7 apparatus in air (30 ml/min) at a linear heating rate of 20°C per min from room temperature to 800°C. The specific surface areas of the samples were determined by BET method using N_2 adsorption/desorption at 77 K on a Carlo Erba Sorptomatic 1990 instrument. The UV-Vis-DRS spectra were recorded on Varian 5E spectrometer with $BaSO_4$ coated integration sphere. The samples were taken in the form of ~2 mm thick self supported pellets to measure the remission function $F(R_\infty)$. The X-band EPR spectra were recorded at 300 K with a Varian E112 EPR spectrometer. Magnetic field was modulated at 100 kHz and the *g*-values were determined with respect to DPPH (2,2′-diphenyl-1-picrylhydrazyl) standard (g = 2·0036). The SEM micrographs were obtained using a JEOL SEM model JSM 5510 microscope. The surface acid–base properties of the catalyst materials were measured by the titration method reported earlier.[13]

The vapour phase transfer hydrogenation of cyclohexanone with isopropanol was carried out in a fixed bed flow glass reactor kept in a hot zone of a vertically set cylindrical furnace. Typically 0·5 g of catalyst was loaded in the middle of the reactor and packed with clean glass beads. The temperature of the reaction was measured by a thermocouple placed in the middle of the catalyst bed. Prior to the reaction, the catalyst was activated in an oxygen flow (30 ml/min) for 3 h at 450°C and then brought to the reaction temperature at 300°C. The reaction mixture was fed through the top of the reactor by means of a motor driven infusion pump (SP2S-MC model, Electronic Corporation, India) with a flow rate of 11·4 g h mol^{-1}. The liquid products were collected in an ice trap and analysed by gas chromatograph (Amil-Nucon 5765, India) using FID and 20% carbowax column. After each run the catalyst was reactivated at 450°C for 3 h in oxygen for the subsequent run. The time-on-stream study of the catalysts was done for a process time of 4 h.

3. Results and discussion

3.1 *TG analysis of the citrate precursor*

In the citrate process, the amorphous solid precursor of a mixed metal oxide, containing all metal ions homogeneously mixed with an organic polyfunctional acid, is prepared by rapid dehydration of a molten mixture of metal salts under low pressure below 100°C. The function of citric acid is to disperse the metal oxide components in the matrix uniformly. In the CeO_2–ZnO preparation, the citrate process produced solid foam during dehydration and continued further expansion of the spongy material when heated in air at 160°C. Figure 1 shows the TGA curve for Ce–Zn–O-cit amorphous precursor measured in air. There is a major weight loss observed between 350 and 550°C due to the decomposition of citrate units to form the final oxide products containing CeO_2. The minor weight changes observed below 300°C are essentially due to the loss of water from the hygroscopic precursors. Further, all the citrate precursors in this study have been calcined at 500°C to obtain the final products.

3.2 *XRD analysis*

The X-ray diffraction patterns of the Ce–Zn–O and ZnO materials prepared by amorphous citrate process and decomposition of the acetate precursors are shown in figure 2. Pure ZnO material prepared by both methods shows intense reflections at

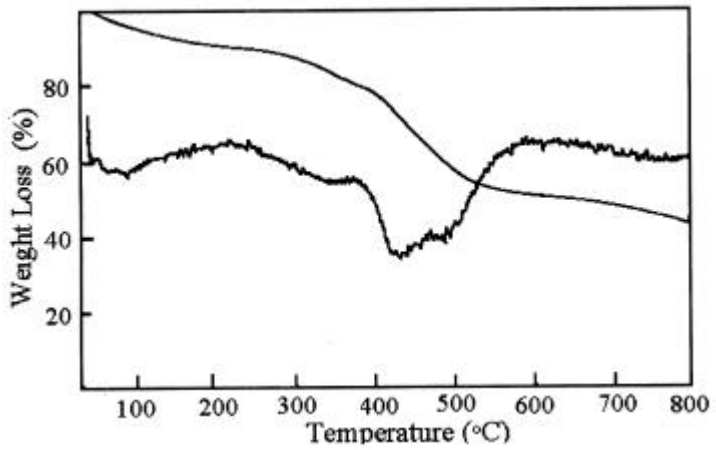

Figure 1. TGA profile of the amorphous citrate precursor, Ce–Zn–O-cit.

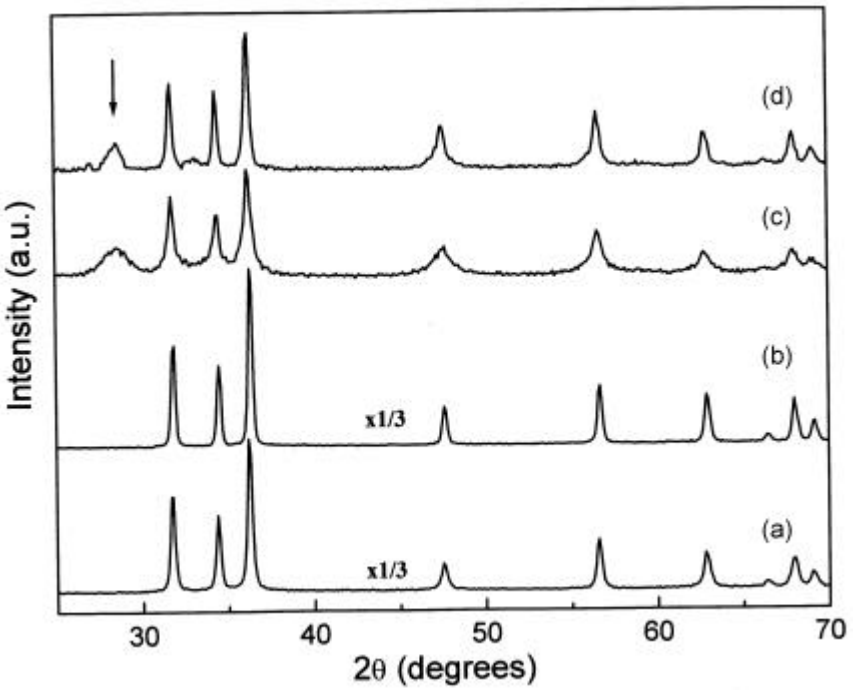

Figure 2. XRD patterns of (a) ZnO-cit, (b) ZnO-dec, (c) Ce–Zn–O-cit and (d) Ce–Zn–O-dec.

2θ = 31·8, 34·4, 36·3, 47·6 and 56·6 corresponding to the Miller indices of (100), (002), (101), (102) and (110) respectively (figure 2a and b). XRD profiles reveal the formation of well-crystalline ZnO in both the preparations. Addition of 10% ceria to the ZnO oxide results in broad and diminished intensities of the ZnO reflections. The new peak at 2θ = 28·7° seen in figure 2c and d corresponds to the (111) reflection of the fluorite structure of the ceria. The broadness of the ceria peak in the both the samples is indicative of the presence of smaller size ceria crystallites in the ZnO matrix. The ceria crystallite sizes calculated by Scherrer's equation[27] are in the range of ~ 150 Å suggesting well-dispersed ceria in the oxide matrix. During the preparation, the citrate precursors retained all the added citric acid as confirmed by the CHN analysis and have shown uniform colouration and homogenous composition. These aspects are significant in the citrate process employed in this study to obtain fine dispersion of nano-range ceria particles in the ZnO matrix.

3.3 *UV-Vis-diffuse reflectance study*

The UV-DRS spectra of the CeO_2–ZnO material along with pure ZnO are presented in figure 3. Pure ZnO-cit shows a broad absorption feature in figure 3a with an absorption edge around 400 nm characteristic of the semiconducting nature of ZnO.[28] Addition of ceria to ZnO changes the absorption features showing new bands in the UV region. Such narrow bands observed in the diffuse reflectance spectra of ceria containing materials

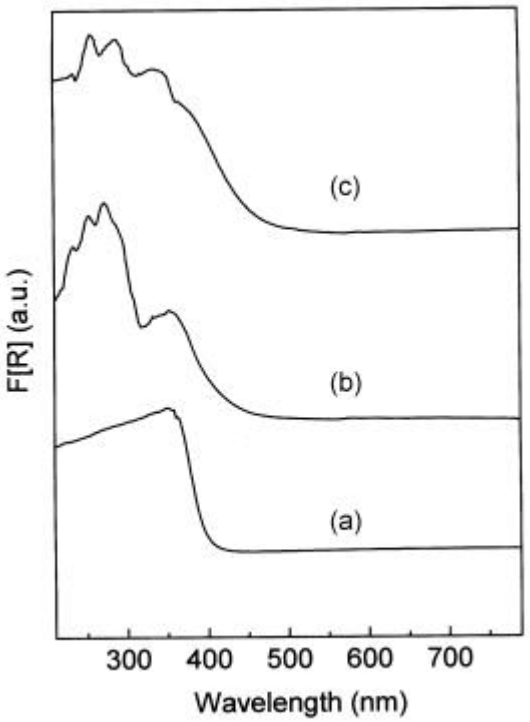

Figure 3. UV-Vis-diffuse reflectance spectra of (a) ZnO-cit, (b) Ce–Zn–O-cit and (c) Ce–Zn–O-dec.

correspond to different interband and charge transfer electronic transitions. UV-DRS spectral features are very sensitive to nano-size oxide particles.[29–31] In addition, the onset of the UV absorption edge depends on the particle size of semiconductor materials such as ceria and ZnO. When crystallite size of CeO_2 is in the nano-range, the band gap energy is inversely related to the crystallite size and hence the absorption edge will be blue shifted.[32] Further the absorption features in the range of 250–350 nm can provide information about the surface species and detect very low concentrations of cerium in a supported powder catalyst. In figure 3b and c, the CeO_2–ZnO samples display four absorption bands at 230, 250–255, 270–285 and 330–345 nm. The later two bands correspond to the $O^{2-} \rightarrow Ce^{4+}$ charge transfer transitions and interband transitions in the CeO_2 crystallite. These characteristic bands have been observed for ceria in highly dispersed state in silica matrix and attributed to localised $O \rightarrow Ce$ charge transfer transitions involving a number of surface Ce^{4+} ions with different coordination numbers.[31,32] The absorption band at 250–255 nm is related to the $O^{2-} \rightarrow Ce^{3+}$ charge transfer transition indicating the presence of lattice imperfection and defect centres on the mixed oxide catalyst. The remaining 230 nm band may be related to the $f \rightarrow d$ transitions of the less populated Ce^{3+} surface species.[31] Therefore the DRS results support the existence of low coordination cerium ions associated with nano-range CeO_2 crystallites.

3.4 *EPR study*

Electron paramagnetic resonance technique has been used for the characterisation of adsorbed paramagnetic species such as superoxide ions and defect centres on the surface of the oxide particles.[33] Pure ZnO with no unpaired electron does not show any EPR signal. However presence of defect centres in the crystal lattice such as anion vacancy

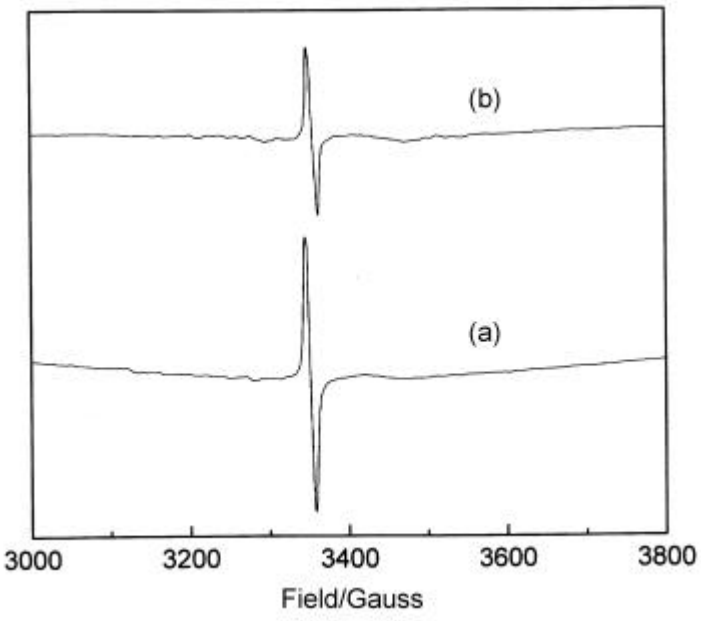

Figure 4. EPR spectra of (a) ZnO-cit and (b) Ce–Zn–O-cit.

followed by the capture of electron can show an EPR signal. The EPR spectra of the ZnO-cit and Ce–Zn–O-cit are shown in figure 4. A symmetric signal was observed at *g* value of 2·0102 (figure 4a) and 2·0096 (figure 4b) respectively. Such EPR signals have been reported for nanometre size ZnO ultrafine particles due to the trapped electron at the O^{2-} vacancies.[34] However, these signals are stable only under ambient conditions and lose intensity at higher temperatures possibly due to the elimination of the defect sites. The *g* values observed for the ZnO-cit and Ce–Zn–O-cit catalyst are in agreement with the reported value[34] and approve the presence of defect sites in Ce–Zn–O materials prepared by citrate process.

3.5 *SEM study*

SEM micrographs of the ZnO-cit and Ce–Zn–O-cit catalysts are shown in figure 5. The SEM micrograph of pure ZnO-cit shows polycrystalline agglomerated particles of irregular shape (figure 5a). Addition of ceria to ZnO catalyst changes the particle morphology and size. The Ce–Zn–O-cit catalyst shows flake like texture and smaller particles (figure 5b). The textural characteristics are due to the swelling nature of the precursors. In the citrate process, the amorphous precursors are prepared by rapid evacuation of the molten mixture of the corresponding salts and citric acid and subsequent heat

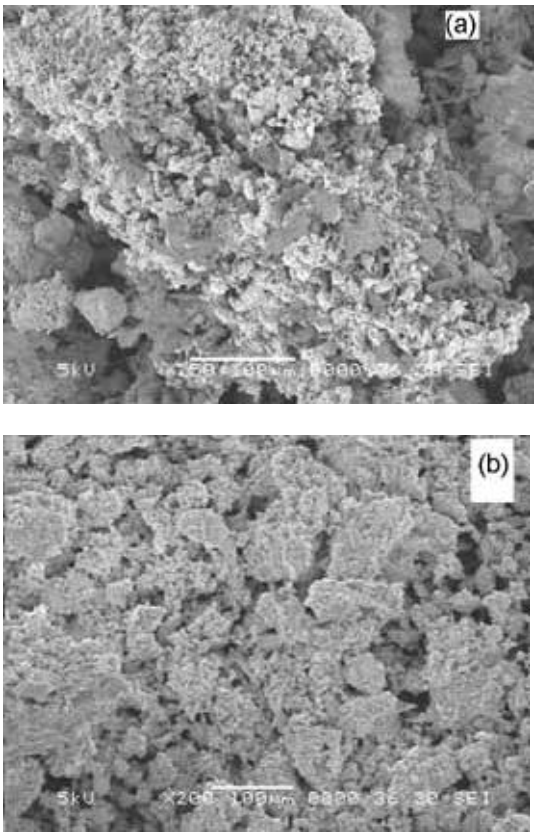

Figure 5. SEM micrographs of (**a**) ZnO-cit and (**b**) Ce–Zn–O-cit.

treatment at 160°C. Considerable swelling of the citrate precursor takes place in the presence of the cerium salts contributing to the mutual dispersion of the oxide components.

3.6 *Catalytic activity*

The activity of Ce–Zn–O-cit catalyst is tested initially for vapour phase transfer hydrogenation of cyclohexanone using 2-propanol as hydrogen donor at 300°C. Cyclohexanol is collected as the sole product of the reaction with selectivity greater than 98%. The reactivity of pure cyclohexanol is checked on the catalyst surface under identical reaction conditions. No appreciable conversion has been observed for cyclohexanol. This eliminates the possibility of further reaction of cyclohexanol via dehydrogenation/ dehydration steps under the reaction conditions. Figure 6 shows the conversion dependence for cyclohexanone on the mole ratio of the feed mixture. It predicts the highest conversion around the cyclohexanone to 2-propanol mole ratio of 1 : 4 on Ce–Zn–O-cit catalyst. Similar result has also been observed for the Ce–Zn–O-dec catalyst. Based on these experiments, we have selected the feed mixture of cyclohexanone to 2-propanol in the molar ratio of 1 : 4 in this study. Table 1 shows the average conversions for ZnO and CeO_2(10%)–ZnO catalysts along with the surface area of the materials prepared by both citrate process and acetate precursor decomposition. The preparative method is found to be important for the physicochemical characteristics of the final catalysts. Addition of ceria in to ZnO is found to increase the surface area in case of the citrate process. This is consistent with earlier reports on CeO_2–MgO mixed oxide materials prepared by the same method.[7,8] The acid–base property of the composite oxides measured by the titration method is also presented in table 1. A good correlation is

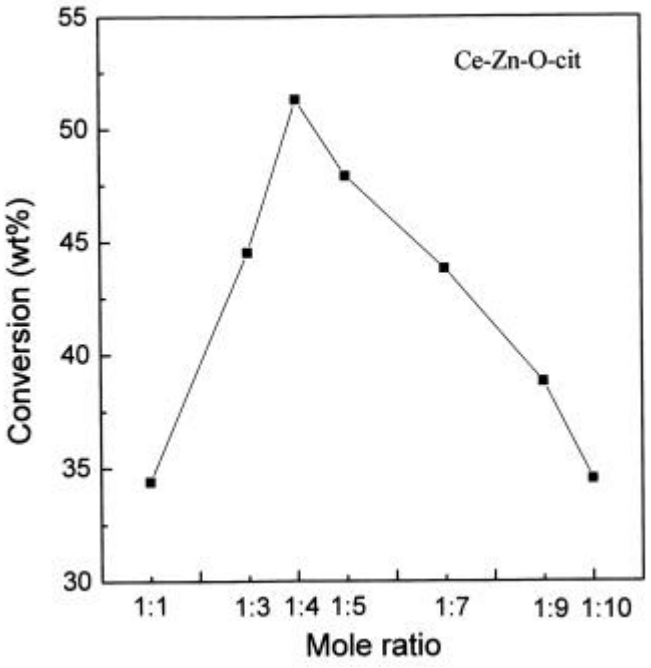

Figure 6. Effect of mole ratio (cyclohexanone : 2-proponol) on the catalytic activity of Ce–Zn–O-cit catalyst at 300°C.

observed between the acid–base properties and the catalytic activity of the Ce–Zn–O composite oxide catalysts. Ceria is an amphoteric oxide with mild acid–base property whereas ZnO is basic in nature.[10] The addition of ceria to ZnO can create new acidic sites with a contribution to the basic character of the composite oxide. The surface acid–base value obtained from the titration method clearly indicates the occurrence of new acidic sites with the addition of ceria. Pure ZnO obtained by either methods show similar acidic and basic properties with slight enhancement from the citrate process. The composite catalysts, on the other hand, show a considerable increase in acidity and a moderate increase in the basic nature. This is in accordance with the earlier observations.[8,11] The

Table 1. The catalytic data obtained for ZnO and Ce–Zn–O samples prepared by the amorphous citrate process and the decomposition of acetate precursors.

Catalyst	Surface area (m^2/g)	Acidity (mmol/g)	Basicity (mmol/g)	Conversion (mol%)
ZnO-dec	10·2	0·032	0·324	17·1
ZnO-cit	15·4	0·038	0·352	21·4
Ce–Zn–O-dec	18·5	0·081	0·384	34·8
Ce–Zn–O-cit	42·1	0·116	0·432	51·3

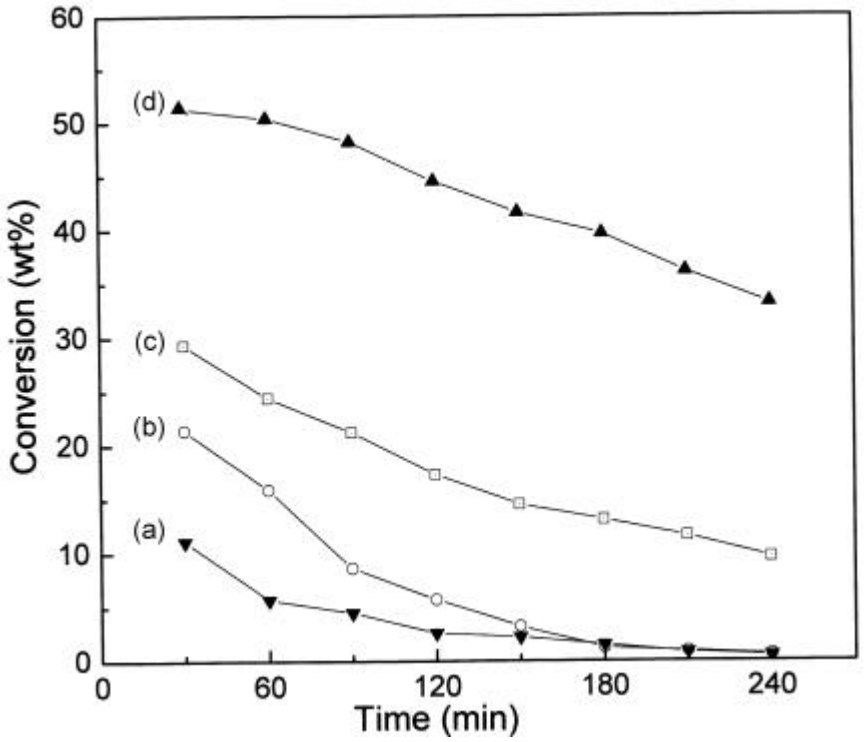

Figure 7. Effect of process time on the catalytic activity of (a) ZnO-dec, (b) ZnO-cit, (c) Ce–Zn–O-dec and (d) Ce–Zn–O-cit.

key factor for the enhancement of acid–base properties of the composite oxides is the dispersion of ceria component in the ZnO matrix. The coordinately unsaturated metal cations and oxygen anions present in the boundary region of the two oxides can contribute to the overall acid–base property of the composite oxides. More number of such sites can be created by employing suitable preparative methods as is the case of the amorphous citrate process. The oxygen mobility and the redox property of the ceria along with the overall acid–base properties appear to be responsible for higher catalytic activity of the composite catalysts. In a similar study, the unusually high activity of ceria containing materials towards the dehydrogenation of alcohols is attributed to the redox properties.[15,35] The formation of isopropoxide species has been detected on the ceria surface by dissociative chemisorption of isoproponol.[35] This species can effectively transfer a hydride ion to the cyclohexanone molecule adsorbed on an adjacent coordinately unsaturated metal ion facilitating the hydrogen transfer process.[13]

Figure 7 shows the conversion versus process time plots for CeO_2–ZnO catalysts. All the catalysts deactivate rapidly with process time. Pure ZnO deactivates rapidly with total loss of catalytic activity after two hour of the reaction. The ZnO-cit catalyst shows slightly higher initial activity compared to the ZnO-dec material but both the samples get deactivated at about the same process time. However, the behaviour of Ce–Zn–O catalysts with time on stream is interesting. They show higher conversions and the rate of deactivation is much slower compared to pure ZnO. As expected from the acid–base and surface area data in table 1, the Ce–Zn–O-cit composite catalyst shows unambiguously higher catalytic activity and is less prone to the deactivation with time on stream compared to the pure ZnO catalyst.

4. Conclusions

Ce–Zn–O mixed oxides are prepared by amorphous citrate process and decomposition of acetate precursors. Ceria crystallites of nanometre range have been dispersed in the ZnO matrix in the Ce–Zn–O composite catalyst prepared by citrate process. UV-DRS and EPR reveal the presence of coordinately unsaturated metal centres and anion vacancies in these oxides. Addition of ceria to ZnO by citrate method influences the particle morphology, surface area and acid–base properties. The activity measurements for hydrogen transfer reaction correlates well with the catalytic data of these materials.

Acknowledgement

Financial support received from the Council of Scientific and Industrial Research, New Delhi, is gratefully acknowledged.

References

1. Kašpar J, Fronasiero P and Graziani M 1999 *Catal. Today* **50** 285
2. Kašpar J, Fornasiero P and Hickey N 2003 *Catal. Today* **77** 419
3. Ranga Rao G, Fornasiero P, Di Monte R, Kašpar J, Vlaic G, Balducci G, Meriani S, Gubitosa G, Cremona A and Graziani M 1996 *J. Catal.* **162** 1
4. Ranga Rao G 1999 *Bull. Mater. Sci.* **22** 89
5. Hoeevar S, Batista J and Levec J 1999 *J. Catal.* **184** 39
6. Cutrifello M A, Ferino I, Solinas V, Primavera A, Trovarelli A, Auroux A and Picciau C 1999 *Phys. Chem. Chem. Phys.* **1** 3369
7. Sato S, Koizumi K and Nozaki F 1998 *J. Catal.* **178** 264

8. Sato S, Takahasi R, Sodesawa T, Matsumoto K and Kamimura Y 1999 *J. Catal.* **184** 180
9. Leclercq E, Rives A, Payen E and Hubaut R 1998 *Appl. Catal.* **A168** 279
10. Mishra B G and Ranga Rao G 2002 *Bull. Mater. Sci.* **25** 155
11. Jyothi T M, Talawar M B and Rao B S 2000 *Catal. Lett.* **64** 151
12. Duprez D and Martin D 1997 *J. Mol. Catal.* **A118** 113
13. Ranga Rao G, Sahu H R and Mishra B G 2003 *React. Kinet. Catal. Lett.* **78** 151
14. Sugunan S and Varghese B 1998 *Indian J. Chem.* **A37** 806
15. Haffad D, Chambellan A and Lavalley J C 2001 *J. Mol. Catal.* **A168** 153
16. Martin D and Duprez D 1996 *J. Phys. Chem.* **A100** 9429
17. Trovarelli A (ed.) 2002 *Catalysis by ceria and related materials* (London: Imperial College Press) p. 1–528
18. Johnstone R A W and Wilby A H 1985 *Chem. Rev.* **85** 129
19. Brieger G and Nestrick T J 1974 *Chem. Rev.* **74** 567
20. Upadhya T T, Katdare S P, Sabde D P, Ramaswamy V and Sudalai A 1997 *J. Chem. Soc., Chem. Commun.* 1119
21. Aramendia M A, Borau V, Jimenez C, Marinas J M, Porras A and Urbano F J 1998 *Appl. Catal.* **A172** 31
22. Kašpar J, Trovarelli A, Lenarda M and Graziani M 1989 *Tetrahedron Lett.* **20** 2705
23. Jyothi T M, Raja T, Sreekumar K, Talawar M B and Rao B S 2000 *J. Mol. Catal.* **A157** 193
24. Joshi M V, Vidya S, Pandey R and Mukesh D 1999 *J. Catal.* **188** 102
25. Szollosi G and Bartok M 1999 *J. Mol. Catal.* **A148** 265
26. Shibagaki M, Takahashi K and Matsushita H 1988 *Bull. Chem. Soc. Jpn.* **61** 3283
27. West A R 1987 *Solid state chemistry and its applications* (New York: John Wiley) p. 174
28. Valenzuela M A, Bosch P, Jimenez-Becerrill J, Quiroz O and Paez A I 2002 *J. Photochem. Photobiol.* **A148** 177
29. Bensalem A, Muller J C and Bozon-Verduraz F 1992 *J. Chem. Soc., Faraday Trans.* **88** 153
30. Weckhuysen B M and Schoonheydt R A 1999 *Catal. Today* **49** 441
31. Ranga Rao G and Sahu H R 2001 *Proc. Indian Acad. Sci.* (*Chem. Sci.*) **113** 651
32. Bensalem A, Bozon-Verduraz F, Delamar M and Bugli G 1995 *Appl. Catal.* **A121** 81
33. Che M and Tench A J 1983 *Adv. Catal.* **32** 1
34. Jing L, Xu Z, Shang J, Sun X, Cai W and Guo H 2002 *Mater. Sci. Eng.* **A332** 356
35. Zaki M I, Hussein G A M, El-Ammawy H A, Mansour S A A, Polz J and Knozinger H 1990 *J. Mol. Catal.* **57** 367